

RESEARCH

Open Access



Positive regulation Asperosaponin VI accumulation by *DaERF9* through JA signaling in *Dipsacus asper*

Huanhuan Yang¹, Jiao Xu^{1,2}, Chunyun Xu¹, Guang Zhou¹, Tao Zhou^{1,2*} and Chenghong Xiao^{1,2*}

Abstract

The ERF transcription factor can regulate the biosynthesis of various secondary metabolites, including triterpenoid saponins, in plants. *DaERF9* has been found to be a potential regulatory factor in the accumulation of asperosaponin VI in *Dipsacus asper*. However, its underlying molecular mechanisms remain unclear. Here, we cloned the transcription factor *DaERF9*, which promotes the accumulation of asperosaponin VI in *D. asper*. Metabolomic analysis showed that wound stress significantly increased the content of asperosaponin VI and jasmonic acid, while the expression level of *DaERF9* was markedly enhanced during this process, suggesting that *DaERF9* plays a regulatory role in the wound-induced synthesis of asperosaponin VI by JA signaling pathway. Transgenic *DaERF9* promoted the synthesis of precursor compounds of asperosaponin VI in *Arabidopsis*, activating the triterpenoid saponin biosynthesis pathway. MeJA induction enhanced the expression of the key enzyme gene *DaHMGR*, which is involved in the synthesis of asperosaponin VI in transgenic *DaERF9*. Wound treatment markedly increased the transcriptional level of *DaERF9* and the content of JA, and *DaERF9* was able to interact with the *DaHMGR* promoter, activating the activity of *DaHMGR*. Overall, our findings suggest that *DaERF9* plays a crucial role in the synthesis of asperosaponin VI in *D. asper* and elucidate the transcriptional regulatory mechanism of JA-induced accumulation of asperosaponin VI.

Keywords *Dipsacus asper*, Asperosaponin VI biosynthesis, ERF TFs, JA signaling pathway, Wounding

Introduction

Dipsacus radix is a traditional Chinese medicinal herb widely used in the field of traditional Chinese medicine. It is primarily employed to treat conditions such as rheumatism, traumatic injuries, and to promote blood circulation and muscle relaxation [1]. In recent years,

increasing research has shown that *Dipsacus radix* not only has significant therapeutic effects in wound healing but also demonstrates unique advantages in disease resistance [2, 3]. In particular, the active compounds in *Dipsacus asper* have exhibited various biological activities in anti-inflammatory, antibacterial, and antiviral effects, providing important evidence for its application in disease treatment [4]. Asperosaponin VI, a key natural active compound in *D. asper*, has significant advantages in disease resistance. Whether in anti-inflammatory, antibacterial, antiviral, immune regulation, or anticancer effects, asperosaponin VI shows powerful pharmacological activity [3, 5, 6].

*Correspondence:

Tao Zhou

taozhou88@163.com

Chenghong Xiao

xiaochenghong1986@126.com

¹Guizhou University of Traditional Chinese Medicine, Guiyang, China

²Guizhou Key Laboratory for Germplasm Innovation and Resource-Efficient Utilization of Dao-di Herbs, Guiyang, China



© The Author(s) 2025. **Open Access** This article is licensed under a Creative Commons Attribution-NonCommercial-NoDerivatives 4.0 International License, which permits any non-commercial use, sharing, distribution and reproduction in any medium or format, as long as you give appropriate credit to the original author(s) and the source, provide a link to the Creative Commons licence, and indicate if you modified the licensed material. You do not have permission under this licence to share adapted material derived from this article or parts of it. The images or other third party material in this article are included in the article's Creative Commons licence, unless indicated otherwise in a credit line to the material. If material is not included in the article's Creative Commons licence and your intended use is not permitted by statutory regulation or exceeds the permitted use, you will need to obtain permission directly from the copyright holder. To view a copy of this licence, visit <http://creativecommons.org/licenses/by-nc-nd/4.0/>.

The synthesis pathway of asperosaponin VI is a multi-step reaction process, involving several steps such as the synthesis of the triterpenoid skeleton, glycosylation modification, and secondary modifications. The skeleton of triterpenoid compounds is typically composed of a C30 carbon chain, and the synthesis process relies on either the mevalonate pathway (MVA) or the methylerythritol phosphate pathway (MEP), with the MVA pathway being the primary route for triterpenoid synthesis [7]. Starting from acetyl-CoA, isopentenyl pyrophosphate (IPP) and dimethylallyl diphosphate (DMAPP) are generated through the catalysis of enzymes such as acetyl-CoA C-acetyltransferase (AACT), 3-hydroxy-3-methylglutaryl-CoA synthase (HMGS), and 3-hydroxy-3-methylglutaryl-CoA reductase (HMGCR) [8]. In this process, isoprene units are polymerized into triterpenoid precursors, and through specific enzymes, such as squalene synthase (SS) and squalene epoxidase (SE), which are key enzymes involved in triterpenoid saponin synthesis, the cyclization reaction is completed to form the triterpenoid skeleton [9]. Existing research suggests that the triterpenoid skeleton of asperosaponin VI is likely derived from precursors such as oleanolic acid or ursolic acid [10]. After the synthesis of the triterpenoid skeleton, further glycosylation reactions form saponins. The glycosylation step of asperosaponin VI relies on sugar sources such as UDP-glucose [11]. The glycosylation process enhances the biological activity of asperosaponin VI, improving its solubility and bioavailability. In the future, optimizing these pathways could increase the yield and activity of asperosaponin VI, thereby promoting its application in drug development and plant protection.

ERF transcription factors play an important role in the synthesis of triterpenoid saponins by regulating the biosynthesis of saponins through the activation or inhibition of genes associated with saponin biosynthesis. *PnERF1*, a positive regulator of triterpenoid saponin biosynthesis in *Panax notoginseng*, can significantly increase the expression levels of genes related to triterpenoid saponin synthesis when overexpressed, thereby increasing the total saponin content [12]. The transcription factor *PjERF1* in *Panax japonicus* has also been found to enhance the synthesis of triterpenoid saponins. Transgenic studies have shown that overexpression of *PjERF1* increases the expression of key biosynthetic genes and significantly enhances the saponin content in the plants [13]. Transcriptome analysis of *Bupleurum falcatum* has shown that transcription factors from the AP2/ERF family are involved in the synthesis of triterpenoid saponins in *Bupleurum*. These factors regulate the expression of genes encoding key enzymes, thereby having a significant impact on the biosynthesis of saponins [14]. Transcriptome analysis in *D. asper* has revealed that the AP2/ERF family may be involved in the jasmonic acid (JA) signaling

pathway, regulating the biosynthesis of asperosaponin VI during its accumulation [15]. However, there are few reports on how ERF transcription factors respond to abiotic stress-induced accumulation of asperosaponin VI.

Plant hormones play an important regulatory role in the synthesis of triterpenoid saponins. Plant hormones such as methyl jasmonate (MeJA), ethylene (ET), and abscisic acid (ABA) influence the synthesis and accumulation of saponin compounds by altering gene expression, enzyme activity, and metabolic flux. Among them, MeJA plays a crucial regulatory role in the synthesis of triterpenoid saponins. In Wang Bu Liu Xing (*Vaccaria segetalis*), UDP-glucose dehydrogenase is affected by MeJA, which alters the oxidation specificity of cytochrome P450 monooxygenases (CYP) toward triterpene glycoside products. This thereby promotes the accumulation of monosaccharide and disaccharide triterpenoid saponins [16]. MeJA can effectively induce the accumulation of ginsenosides Rb1, Rc, Rb2, Rb3, and notoginsenosides Fa and Fe in *Panax notoginseng* leaves. It enhances the high expression of genes such as *PnFPS*, *PnSS*, *PnSE*, *PnDS*, and *PnUGTs*, thereby promoting the biosynthesis of PPD-type saponins [14]. In *Panax ginseng*, after treating cell suspension cultures with MeJA, three ginsenosides (Rg1, Re, and Rb1) were detected. After 72 h, the total saponin content reached four times that of the control group, indicating that MeJA significantly increased the synthesis of saponins [17]. Transcriptome analysis revealed that the levels of JA and its related metabolites significantly increased during root development. And the accumulation of asperosaponin VI was detected in the root tip, indicating that the biosynthesis and signaling of JA are closely associated with the biosynthesis of asperosaponin VI [15].

Mechanical damage can induce plant defense responses, including the synthesis of triterpene saponins, in which specific transcription factors play a key role. In *Medicago truncatula*, two jasmonic acid-induced bHLH family transcription factors, *MtTSAR1* and *MtTSAR2*, have been found to directly regulate the biosynthesis of triterpene saponins. These transcription factors activate the expression of *MtHMGR1* by binding to the N-box on its promoter, thereby promoting the synthesis of triterpene saponins [18]. In studies of *Panax notoginseng*, the transcription factor *PnbHLH1* has been shown to positively regulate the biosynthesis of triterpene saponins. Overexpression of *PnbHLH1* significantly increases the expression levels of key triterpene saponin genes, *PnDS*, *PnSS*, and *PnSE*, thereby enhancing the yield of saponins [19]. In *Salvia miltiorrhiza*, the two ERF family transcription factors, *SmERF6* and *SmERF8*, can directly bind to the promoter regions of key enzyme genes in the tanshinone biosynthesis pathway, promoting their expression and thereby increasing the accumulation of tanshinones

[13]. These studies suggest that transcription factors enhance plant defense responses to mechanical injury by regulating the biosynthesis of triterpene saponins, thereby boosting the plant's defensive capacity.

Our research group previously identified *DaERF9*, an MeJA-induced ERF transcription factor in *D. asper*. Given that MeJA treatment promotes asperosaponin VI synthesis, we hypothesize that *DaERF9* plays a key role in regulating this process [22]. In this study, we cloned the *DaERF9* gene and performed functional analysis, revealing that it is a wounding-responsive gene. *DaERF9* binds to and activates the expression of *DaHMGCR*, thereby promoting the biosynthesis of asperosaponin VI under mechanical injury conditions. Our findings provide new insights into the function of ERF transcription factors in the wounding-induced synthesis of asperosaponin VI.

Materials and methods

Plant materials and stress treatments

The sources of the plants, seeds, and plant materials involved in this study are as follows: Seeds of *D. asper*: The seeds were collected from Longli County, Guizhou Province, and were identified as *D. asper* by Prof. Xiao Chenghong. And is deposited at the Medicinal Herbarium, Guizhou University of Traditional Chinese Medicine (Collection Number: GZTM0220136). All *D. asper* plants in this study were grown from these seeds. *Arabidopsis thaliana*: Columbia ecotype of *Arabidopsis thaliana* was used. *Nicotiana benthamiana*: *Nicotiana benthamiana* plants were employed.

D. asper seeds were sown in seedling trays filled with moist organic nutrient soil and placed in a light-controlled growth chamber at 22 °C (with a 16-hour light/8-hour dark cycle) for 2 weeks to obtain *D. asper* seedlings. After transplantation into flower pots, the seedlings were cultivated for an additional 4 weeks before being used for the following experiments.

The *D. asper* seedlings were transplanted to the experimental field, and roots were collected at 1, 3, 6, 12, and 24 months after transplantation. After 2 years of transplantation, when 60% of the plants had open capitata inflorescences and 10% had begun to bear fruits, samples including leaves, roots, stems, flowers, petioles, and seeds were collected during the flowering and fruiting period. For sample collection, 15 *Astragalus membranaceus* plants were selected, randomly grouped into three replicates, with 5 plants per replicate. The samples were rapidly frozen in liquid nitrogen and stored in a low-temperature freezer for gene expression analysis at different time points and tissues.

In the mechanical injury induction experiment, *D. asper* was grown in hydroponic trays for 45 days (in a 22 °C growth chamber with a 16-hour light/8-hour dark cycle). The leaves of the *D. asper* plants were subjected

to damage treatment using a 1 ml syringe with the needle removed. Samples were collected at 6 h, 12 h, 1 day, and 3 days after treatment. The leaves were used for gene expression analysis and physiological index measurement, while both leaves and roots were used for metabolite content measurement. The experiment was repeated.

The tobacco used was *Nicotiana benthamiana*, grown at 22 °C (with a 16-hour light/8-hour dark cycle) for 1 month for subcellular localization and dual luciferase reporter gene experiments. The *Arabidopsis thaliana* used was of the Columbia type, grown at 22 °C (with a 16-hour light/8-hour dark cycle) in a light-controlled growth chamber until the floral buds just began to open, and was used for gene transformation.

RNA extraction and *DaERF9* gene cloning

The roots of *D. asper* seedlings were harvested, RNA was extracted, and reverse transcription was performed for gene cloning. The total RNA extraction method was performed according to the instructions provided in the Eastep® Super Total RNA Extraction Kit manual (Pomega). RNA concentration and purity were measured using a low volume nuclei acid and protein analyzer (Implen, Germany). RNA degradation and contamination were assessed via 1.2% agarose gel electrophoresis. The quality of the RNA was determined based on these analyses. The total RNA was then reverse transcribed into cDNA following the instructions of the Takara Prime Script™ RT reagent Kit (Perfect Real Time). The cDNA was stored at -20 °C for future use.

The cloning primers were designed using Premier 5 software. The upstream primer was *DaERF9*-F: 5'- TCT CTCAAACACATACACACTAACATCT -3', and the downstream primer was *DaERF9*-R: 5'- TGCACATA AACGGTGATCATTG -3', synthesized by Shanghai Sheng Gong Sequencing Company. PCR amplification was performed using the cDNA synthesized by reverse transcription as the template. The PCR product was checked by 1.2% agarose gel electrophoresis. The product was then ligated into the pMD19-T Vector and transformed into TOP10 competent cells. The cells were plated on LB solid media containing 100 mg/L ampicillin and incubated at 37 °C for 12 h. Positive clones were selected and cultured in LB liquid media (with 100 mg/L ampicillin) at 37 °C with shaking for 6 h. PCR detection of the bacterial culture was performed, and positive clones were sent for sequencing at Shanghai Sheng Gong Sequencing Company.

qRT-PCR analysis

The materials for qRT-PCR analysis of different tissues were the roots, stems, leaves, petioles and seeds of *D. asper*. The samples of different growth and development periods were the *D. asper* roots of 1 month, 3 months, 6

months, 12 months and 24 months. RNA was extracted from the above samples and reverse-transcribed for qRT-PCR analysis. Using Primer 5.0 software for real-time fluorescence quantitative primer design, the primers were synthesized by Shanghai Sangon Biotech Co., Ltd., and the primer sequences are provided in Table S1. *Daactin103* was used as the internal reference gene [15], and RT-qPCR was used to detect the relative gene expression levels in *D. asper*. The internal reference for *Arabidopsis* was *Atactin* [20]. RT-qPCR reaction system (10 μ L): 5 μ L TB Green™ premix Ex Taq™ II, 0.5 μ L of forward and reverse primers each, 4 μ L of cDNA template. The results were analyzed using the $2^{-\Delta C_t}$ method [15].

Subcellular localization

The cloned *DaERF9* gene was fused with the pCOA30-GFP vector plasmid through homologous recombination, with restriction enzymes *Pst*I and *Bam*HI used for digestion. Subsequently, the fusion vector *DaERF9*-pCOA30-GFP and pBI121-NLS-mCherry were respectively transformed into *Agrobacterium tumefaciens* competent cells GV3101. After shaking culture and resuspension, the mixed bacterial solution of the two was injected into the leaves of *Nicotiana benthamiana* using a needleless syringe. After dark incubation for 24 h, followed by normal incubation for 36 h, the *Nicotiana benthamiana* leaves were subjected to fluorescence detection under a laser confocal microscope. Observation was carried out by means of a laser scanning confocal microscope (Zeiss LSM900). Confocal parameters: pCOA30-GFP: excitation wavelength 488 nm, emission wavelength 507 nm; pBI121-NLS-mCherry: excitation wavelength 561 nm, emission wavelength 610 nm; peak width \pm 10 nm.

Establishment of the overexpression *DaERF9* genetic system

Using the method of homologous recombination, the vector was digested with restriction enzymes *Nco*I and *Eco*RI to construct the 35 S::*DaERF9*-pCAMBIA3301 overexpression vector. After successful sequencing, the vector was transformed into *Agrobacterium tumefaciens* GV3101 competent cells. Following PCR detection of the bacterial solution, positive single colony cultures were selected for *Arabidopsis* genetic transformation, with slight adjustments made to the floral dip method [21]. A small amount of positive bacterial solution was transferred to YPDA liquid medium (with kanamycin and rifampicin antibiotics) for activation. The bacterial solution was cultured to increase its volume, bringing the OD600 to approximately 0.8–0.9. The bacterial solution was then adjusted to an OD600 of 0.6 using a 5% sucrose solution, and incubated at room temperature, away from light, for 1 h. Wild-type *Arabidopsis thaliana* plants,

grown under 22 °C light conditions (16 h light/8 hours dark), had their open flowers and mature pods removed, leaving only the newly exposed inflorescences and flower buds. The inflorescences were immersed in the *Agrobacterium* suspension for 2 min, excess bacteria were blotted off, and the plants were incubated in the dark at 22 °C for 24 h before being returned to normal light conditions (22 °C, 16 h light/8 hours dark). After one week, the transformation was repeated to obtain infected *Arabidopsis thaliana* plants.

After the *Arabidopsis thaliana* seeds from the infected plants mature, they are collected and dried to obtain T0 generation seeds. The T0 seeds are disinfected and sown onto moist organic nutrient soil under a 16-hour light/8-hour dark cycle at 22 °C. Basta solution is used to screen for resistant plants. The healthy, resistant *Arabidopsis thaliana* seedlings are selected as T1 generation plants. A few 1–2 leaves from the T1 *Arabidopsis thaliana* plants are collected, and cDNA is extracted and reverse-transcribed using a kit. PCR is then performed for positive identification and screening. The positive plants are further cultivated to harvest T1 generation seeds. Basta solution is again used for resistance screening of T1 generation seeds, and the T2 generation transgenic *Arabidopsis thaliana* plants are obtained for further study.

DaERF9-OE and wounding metabolite content detection in *D. asper*

The transgenic samples are the roots of T2 generation transgenic *DaERF9 Arabidopsis thaliana*, while the control group consists of wild-type *Arabidopsis thaliana* roots. The mechanical injury detection samples are the leaves and roots of *D. asper* three days after mechanical injury, with the control group consisting of untreated *D. asper* leaves and roots.

100 mg of the aforementioned samples were placed in 2 mL centrifuge tubes, with one 6 mm diameter grinding bead added. 800 μ L of extraction solution (methanol: water = 4:1 (v: v)) containing four internal standards (e.g., L-2-chlorophenylalanine at 0.02 mg/mL) was added for metabolite extraction. The samples were then ground for 6 min using a cryogenic tissue grinder (-10 °C, 50 Hz), followed by low-temperature ultrasonic extraction for 30 min (5 °C, 40 kHz). The samples were allowed to sit at -20 °C for 30 min and then centrifuged for 15 min (4 °C, 13,000 g). The supernatant was transferred to an injection vial with an insert for analysis. The LC-MS analysis was conducted using Thermo Fisher's ultra-high-performance liquid chromatography coupled with Fourier transform mass spectrometry UHPLC-Q Exactive system. The chromatography conditions were as follows: The C18 column was ACQUITY UPLC BEH C18 (100 mm \times 2.1 mm i.d., 1.7 μ m; Waters, Milford, USA). The mobile phase A was 2% acetonitrile in water (with 0.1% formic

acid), and mobile phase B was acetonitrile (with 0.1% formic acid). The injection volume was 3 μ L, and the column temperature was set to 40 °C. The analysis was performed by Shanghai Meiji Biological Pharmaceutical Technology Co., Ltd., and the data was processed using the Meiji Bio Cloud Platform (cloud.majorbio.com).

Gene expression analysis of *DaERF9*-OE and wounding in *D. asper*

After disinfecting the T2 generation transgenic *Arabidopsis* seeds, they were suspended in 1% agar and spread onto MS solid medium to germinate. After two true leaves had grown, the seedlings were transplanted. Some of the transgenic seedlings were transplanted into flower pots filled with moist organic nutrient soil and placed in a light incubator (2 °C, 16 h light/8 hours dark). Roots were collected just before bolting for gene expression analysis. Other transgenic seedlings were transplanted into seedling trays filled with vermiculite, supplemented with hydroponic solution, and placed in the light incubator for 1 month (22 °C, 16 h light/8 hours dark). A 150 μ mol/L MeJA solution was sprayed, and after 3 days, the roots were collected for gene expression analysis. The remaining transgenic seedlings were transplanted into MS solid medium and placed in a greenhouse (22 °C) for 14 days, followed by 7 days at 4 °C for low-temperature treatment and then 3 days of recovery. The roots were collected for gene expression analysis. The detection method was the same as described in Sect. 2.3, and the primer sequences are listed in Table S1.

Wounding injury *D. asper* RNA extraction was performed as described in Sect. 2.2, and the detection method was the same as in Sect. 2.3. The primer sequences are listed in Table S1.

Measurement of activity of antioxidant enzymes

For the analysis of physiological indicators in *D. asper* leaves, 0.1 g of leaf tissue was thoroughly ground using liquid nitrogen and placed in an enzyme-free centrifuge tube for detection.

Peroxidase (POD) Activity: POD enzyme activity was detected using the POD activity detection kit (Solebao, Beijing) according to the manufacturer's instructions. To 0.1 g of leaf powder, 1 mL of POD extraction solution was added and homogenized in an ice bath. The mixture was centrifuged at 8000 g at 4 °C for 10 min. The supernatant (5 μ L) was placed in a microplate, and 240 μ L of POD detection solution was added (Reagent 1: 120 μ L, Reagent 2 working solution: 30 μ L, Reagent 3: 30 μ L, distilled water: 60 μ L). The mixture was immediately mixed and timed, and the absorbance was measured at 470 nm for 30 s (A1) and 1 min 30 s after mixing (A2). The change in absorbance was calculated as $\Delta A = A2 - A1$. POD activity (U/g weight) = $9800 * \Delta A / W$, where W is the sample

weight. Each sample was tested in triplicate with three biological repeats.

Superoxide Dismutase (SOD) Activity: SOD enzyme activity was detected using the SOD activity detection kit (Solebao, Beijing) according to the manufacturer's instructions. To 0.1 g of leaf powder, 1 mL of SOD extraction solution was added and homogenized in an ice bath. The mixture was centrifuged at 8000 g at 4 °C for 10 min. The supernatant (20 μ L) was mixed with Reagents 1 (45 μ L), Reagent 2 working solution (20 μ L), Reagent 3 (35 μ L), distilled water (70 μ L), and finally Reagent 4 working solution (10 μ L). The control group and blank group were set up, with the control group lacking Reagent 2 working solution, and blank group 1 and blank group 2 lacking the supernatant and Reagent 2 working solution, respectively. After all reagents were added, the mixture was thoroughly mixed and incubated at 37 °C for 30 min. The absorbance was measured at 450 nm. The change in absorbance for the sample was calculated as $\Delta A_{\text{sample}} = A_{\text{sample}} - A_{\text{control}}$, and the change in the blank as $\Delta A_{\text{blank}} = A_{\text{blank1}} - A_{\text{blank2}}$. The inhibition percentage was calculated as $(\Delta A_{\text{sample}} - \Delta A_{\text{blank}}) / \Delta A_{\text{blank}} * 100\%$. SOD activity (U/g weight) = $10 * \text{inhibition percentage} / (1 - \text{inhibition percentage}) / W$, where W is the sample weight. Each sample was tested in triplicate with three biological repeats.

Malondialdehyde (MDA) Detection: MDA content was detected using the lipid oxidation (MDA) detection kit (Biyuntian, Shanghai). To 0.1 g of leaf powder, 1 mL of IP cell lysis solution (P0013) was added and homogenized in an ice bath. The mixture was centrifuged at 12,000 g at 4 °C for 10 min. The supernatant (100 μ L) was mixed with 200 μ L of MDA detection working solution. A blank control was set with 100 μ L of IP cell lysis solution, and standard samples with concentrations of 1, 2, 5, 10, 20, and 50 μ M were used to generate a standard curve. After mixing the solution, the sample was heated in a boiling water bath for 15 min, then cooled to room temperature, and centrifuged at 1000 g for 10 min. The supernatant (200 μ L) was transferred to a 96-well plate, and absorbance was measured at 532 nm. The MDA content was calculated based on the standard curve. Each sample was tested in triplicate with three biological repeats.

DaHMGCR promoter cloning

Based on the cDNA sequence of the *DaHMGCR* gene from *D. asper* and the amplification primers obtained in previous studies by the research group, genomic sequence verification was performed. Genome Walking technology was used for genomic DNA sequence cloning. Specific primers SP1, SP2, and SP3 were designed to target known sequences and amplify the unknown flanking sequences of the gene. These primers were used in three rounds of specific amplification, following

the instructions provided by the Genome Walking Kit. After performing the amplification, clear PCR bands were selected, and the corresponding PCR products were purified and ligated into the pMD™19-T vector. Positive bacterial cultures were then confirmed by PCR, and the plasmid DNA was sent to Shanghai Sangon Biotech Co., Ltd. for sequencing.

Luciferase assay

Based on the sequencing results, specific upstream and downstream primers were designed for PCR amplification. The amplified PCR products were then ligated into the pGreenII 0800-LUC vector using the ClonExpress II One Step Cloning Kit. The vector was digested with restriction enzymes PstI and BamHI. The following engineered plasmids were obtained: DaERF9::LUC and Pro-DaHMGCR::LUC. The constructed plasmids were then mixed with the pSOUP plasmid and introduced into *Agrobacterium tumefaciens* GV3101 competent cells to obtain the engineered strain for tobacco transient transformation. Tobacco plants (*Nicotiana benthamiana*) that were 1 month old, healthy, and of uniform growth were selected for *Agrobacterium* injection. The abaxial side of the selected tobacco leaves was marked with the injection area. A 1 mL sterile syringe was used to slowly inject the bacterial solution into the marked area until the solution was fully infiltrated. After the injection, the tobacco plants were placed back into a controlled environment chamber for dark incubation for 48–72 h. After the incubation period, the leaves were sprayed with 0.5 mM D-luciferin potassium salt and immediately placed in the dark for a 10-minute reaction. Following the reaction, the LUC fluorescence images were captured using a chemiluminescence/fluorescence imaging system (Tanon-5200, China).

Y1H

To study the role of the GCC-box element in the promoter region, fragments containing the GCC-box sequence were isolated. The core GCC-box sequence, along with 20 bp of upstream and downstream flanking sequences, was extracted. A 45 bp fragment was selected and inserted into the pLacZi vector, which contains the LacZi reporter gene. The DaERF9 gene was then subcloned into the pB42AD vector downstream of the AD domain. Both plasmids were co-transformed into *Saccharomyces cerevisiae* EGY48 competent cells. The transformed cells were plated on SD/-Trp-Ura selection plates and incubated at 30 °C for 48 h. After incubation, five colonies from each experimental group with good growth were selected and cultured in the dark at 30 °C for 2–3 days to observe the color reaction. The results were recorded by taking photographs of the colonies to document the color development.

Other statistical methods

Statistical analysis of the experimental data was performed using IBM SPSS Statistics 26 software, while graphs were generated and processed using Origin 2024 and Graphpad Prism9.5. The results are presented as means ± standard error (SE). Significant differences between groups ($P \leq 0.05$) were determined using one-way analysis of variance (ANOVA) followed by Duncan's multiple range test.

Results

DaERF9 response to MeJA induction

In previous studies conducted by the research group, it was found that the DaERF9 gene clustered together with stress-related genes *PtrERF9*, *AtERF6*, *AtERF59*, *PtrERF108*, and *AT5G511901* into a single group (Supplemental Fig. 1a), suggesting that DaERF9 may play a role in responding to environmental stress. At the same time, the content of asperosaponin VI in *D. asper* significantly increased after MeJA treatment (Supplemental Fig. 1b). Further expression analysis revealed that the expression of DaERF9 was significantly upregulated under MeJA induction (Supplemental Fig. 1c), indicating that the gene may respond to MeJA induction and help resist environmental stress.

Expression analysis and subcellular localization of DaERF9

The expression level of DaERF9 was detected by qRT-PCR to analyze its expression pattern in *D. asper*. The results showed that DaERF9 had the highest expression level in the leaves of *D. asper*, significantly higher than in other organs, followed by expression in the petioles and roots (Fig. 1a). In the roots of *D. asper* at different developmental stages, the expression level in 24-month-old roots was significantly higher than in other stages (Fig. 1b). Subcellular localization analysis indicated that DaERF9 was expressed in the nucleus (Fig. 1c). Based on these results, it is speculated that DaERF9 may primarily regulate the synthesis of asperosaponin VI in the leaves, and later in the growth stages, it may be transferred to the roots for accumulation.

Overexpression of DaERF9 promotes the accumulation of Asperosaponin VI precursors

qRT-PCR analysis of DaERF9 expression in transgenic *Arabidopsis* showed that, compared to the wild-type, the expression levels of DaERF9 were significantly elevated in all three transgenic lines, indicating the successful establishment of the DaERF9 overexpression lines (Fig. 2a). Ultra-high performance liquid chromatography-tandem mass spectrometry (UHPLC-MS/MS) identifying and annotating 681 chemical composition. There are 113 secondary metabolic components, including terpenoids, flavonoids, phenolic acids, indoles, organic

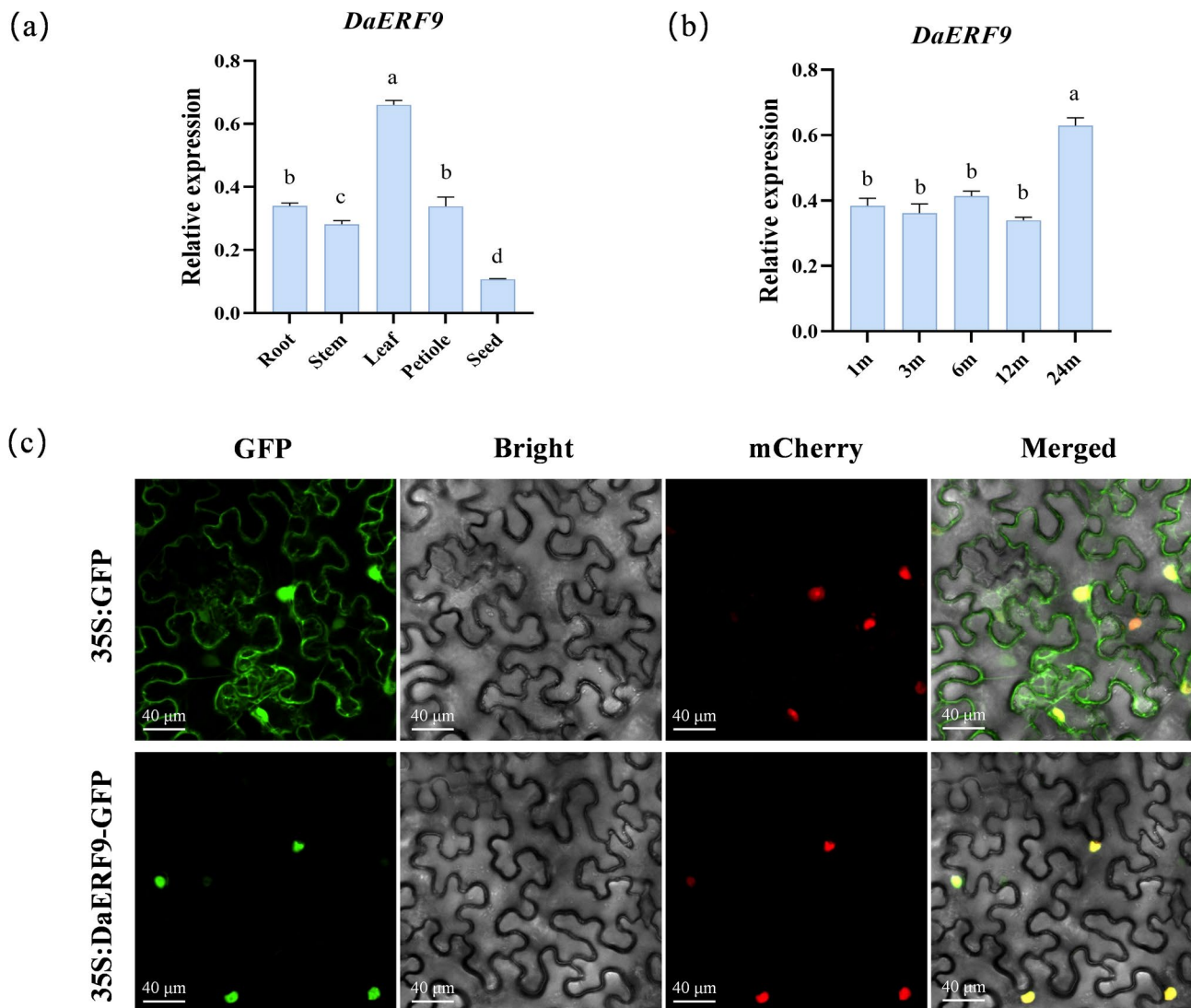


Fig. 1 *DaERF9* expression analysis and Subcellular Localization. **(a)** Expression pattern in different tissues. **(b)** Expression pattern at different growth stages. **(c)** Subcellular localization analysis. Data represent the values of the mean \pm SE (standard error) of three replicates. Note Different lowercase letters indicate significant differences between treatments under the same indicator ($p < 0.05$)

acids, coumarins, steroids, alkaloids, lignans, quinones, anthraquinones, and their respective derivatives (Supplemental Fig. 2). Based on the characteristics of secondary metabolites, the overexpression samples of *DaERF9* and the wild-type samples clearly form two distinct clusters (Supplemental Fig. 3). Among the differential metabolites, terpenoid compounds were the most abundant, with a total of 82, of which 55 were upregulated and 27 downregulated compared to the wild-type. Notably, 13 triterpenoid compounds were upregulated, while 1 was downregulated (Fig. 2b). While most monoterpenes, sesquiterpenes, and diterpenes also exhibited upregulation, a subset of these compounds showed downregulation (Fig. 2c). VIP analysis revealed that the VIP scores of all triterpenes were greater than 1, and the top 10 metabolites were entirely composed of triterpenes (Fig. 2d). This

suggests that triterpenoid compounds are the primary contributors to the metabolic differences between the transgenic *Arabidopsis* and wild-type plants. Among the significantly upregulated triterpenoids, oleanolic acid, soyasapogenol E, glycyrrhetic acid, and maslinic acid belong to the oleanane-type pentacyclic triterpenoids, which exhibit a shared backbone structure with asperosaponin VI. Notably, oleanolic acid, serving as a precursor for the synthesis of asperosaponin VI, demonstrated the highest VIP value of 1.92, thereby contributing most substantially to the observed metabolic variations (Fig. 2d). Its content accumulated significantly, being 1.3 times higher than that in the wild-type (Fig. 2e). These results suggest that *DaERF9* significantly promotes the accumulation of asperosaponin VI precursor compounds in the *Arabidopsis* plants.

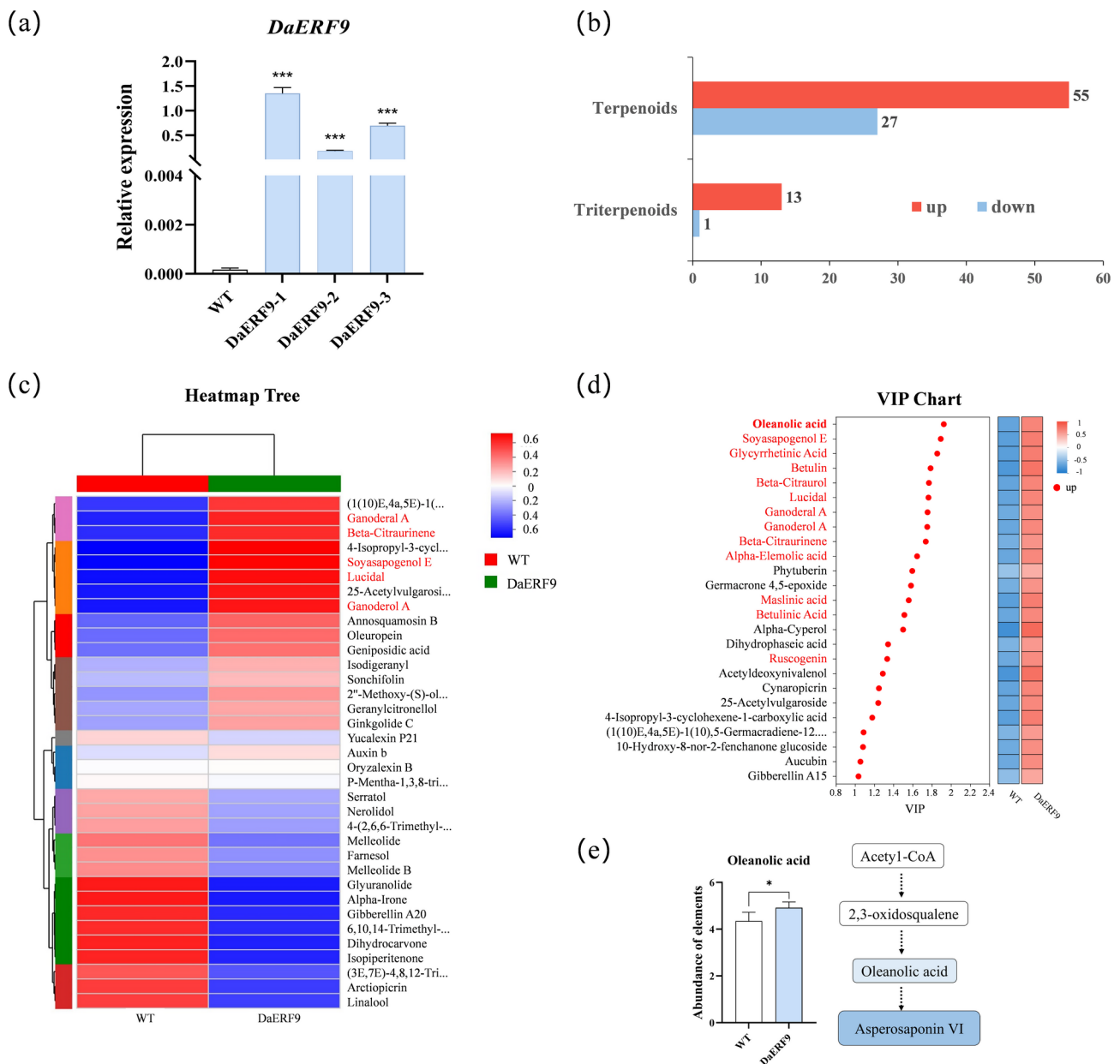


Fig. 2 Metabolite content detection in *DaERF9* overexpressing. **(a)** Expression level of *DaERF9* in *DaERF9* overexpressing plants. **(b)** Differences in terpenoid metabolites in *DaERF9* overexpressing plants. **(c)** Clustering analysis of terpenoid metabolites in *DaERF9* overexpressing plants. The heat map represents metabolites whose abundance is up-regulated, and blue represents metabolites whose abundance is down-regulated. The red letters are triterpenoids. **(d)** VIP bar chart of terpenoid components. The heat map represents metabolites whose abundance is up-regulated, and blue represents metabolites whose abundance is down-regulated. The red letters are triterpenoids. **(e)** Content of asperosaponin VI synthesis precursor compounds. Red font metabolites are triterpenoid components. Data represent the values of the mean \pm SE (standard error) of three replicates. Note Different lowercase letters indicate significant differences between treatments under the same indicator ($p < 0.05$)

Overexpression of *DaERF9* activates the triterpene biosynthetic pathway and responds to MeJA induction

qRT-PCR analysis demonstrated that in *DaERF9*-overexpressing *Arabidopsis*, the expression of upstream genes *AtHMGS* and *AtHMGR* in the terpenoid biosynthesis pathway increased by 2.2-fold and 3.0-fold, respectively, compared to wild-type plants. Similarly, downstream genes *AtSS* and *AtSE* were upregulated by 1.3-fold and

2.1-fold, respectively (Fig. 3a). This suggests that overexpression of *DaERF9* can activate the triterpene biosynthetic pathway, contributing to the synthesis of triterpene compounds in *Arabidopsis*. It is speculated that the *DaERF9* gene plays an active role in the biosynthesis of asperosaponin VI.

After MeJA treatment, compared with the wild type, the key enzyme-encoding genes *AtAACT*, *AtHMGS*,

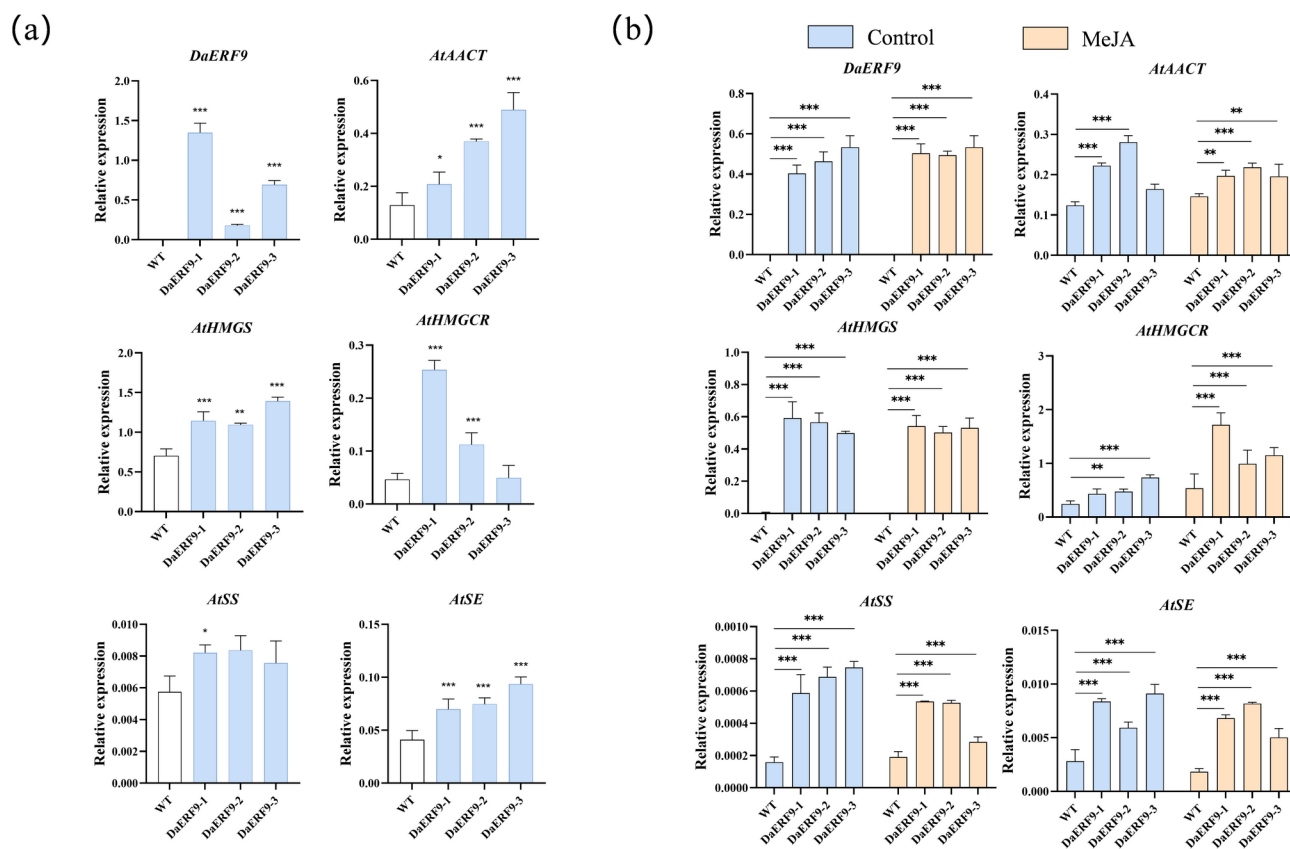


Fig. 3 Gene expression analysis of terpenoid biosynthetic pathway in *DaERF9* overexpressing Arabidopsis. **(a)** Relative expression levels of key enzyme genes in the terpenoid biosynthesis pathway. **(b)** Gene expression analysis of terpenoid biosynthetic pathway genes after MeJA treatment. Data represent the values of the mean \pm SE (standard error) of three replicates. Note Different lowercase letters indicate significant differences between treatments under the same indicator ($p < 0.05$)

AtHMGCR, and *AtSS* in the triterpene biosynthesis pathway exhibited significant upregulation in the samples overexpressing *DaERF9*. Compared to the untreated samples, following MeJA treatment, no significant differences were observed in the expression levels of genes such as *AtAACT*, *AtHMGs*, *AtSS*, and *AtSE*. However, MeJA treatment markedly increased the expression level of the *AtHMGCR* gene, with its expression approximately doubling that of the control group (Fig. 3b). These results confirm that the *DaERF9* gene can activate the terpenoid biosynthesis pathway, respond to MeJA induction, and subsequently regulate the synthesis of terpenoid compounds.

Wounding promotes the synthesis of Asperosaponin VI in *D.asper*

Physiological index detection revealed that after mechanical injury, the activities of POD and SOD enzymes in the leaves of *D.asper* significantly increased, while the malondialdehyde (MDA) content also accumulated significantly. As the injury time increased, the activities of POD and SOD enzymes and the MDA content showed a decreasing trend (Supplemental Fig. 4). These findings

indicate that the cell membrane system of *D.asper* cells suffered oxidative damage under mechanical stress, leading to adverse environmental pressure on the seedlings. However, over time, the plants gradually adapted to this environmental stress and developed resistance.

The analysis of secondary metabolites in the leaves and roots of *D. asper* revealed significant differences in metabolic profiles between leaves and roots before and after mechanical damage (Fig. 4a). A clustering analysis of terpenoid compounds showed that the metabolites mainly clustered into two major categories, with significant differences in the leaves and roots of *D. asper* before and after mechanical injury (Fig. 4b). A statistical analysis of 27 triterpenoid compounds in the leaves revealed that 16 metabolites with VIP values > 1 were differentially expressed, with 9 compounds upregulated after mechanical injury. Among the upregulated compounds, the pentacyclic triterpenoid compounds included Asperosaponin V, Lucyoside N, Soyasaponin II, Beta-elemenic acid, Oleanolic acid, and 28-[Glucosyl-(1 \rightarrow 6)-glucosyl] oleanolic acid 3-arabinoside. Notably, asperosaponin VI and its precursor Oleanolic acid had significantly higher concentrations in the injured samples compared to the

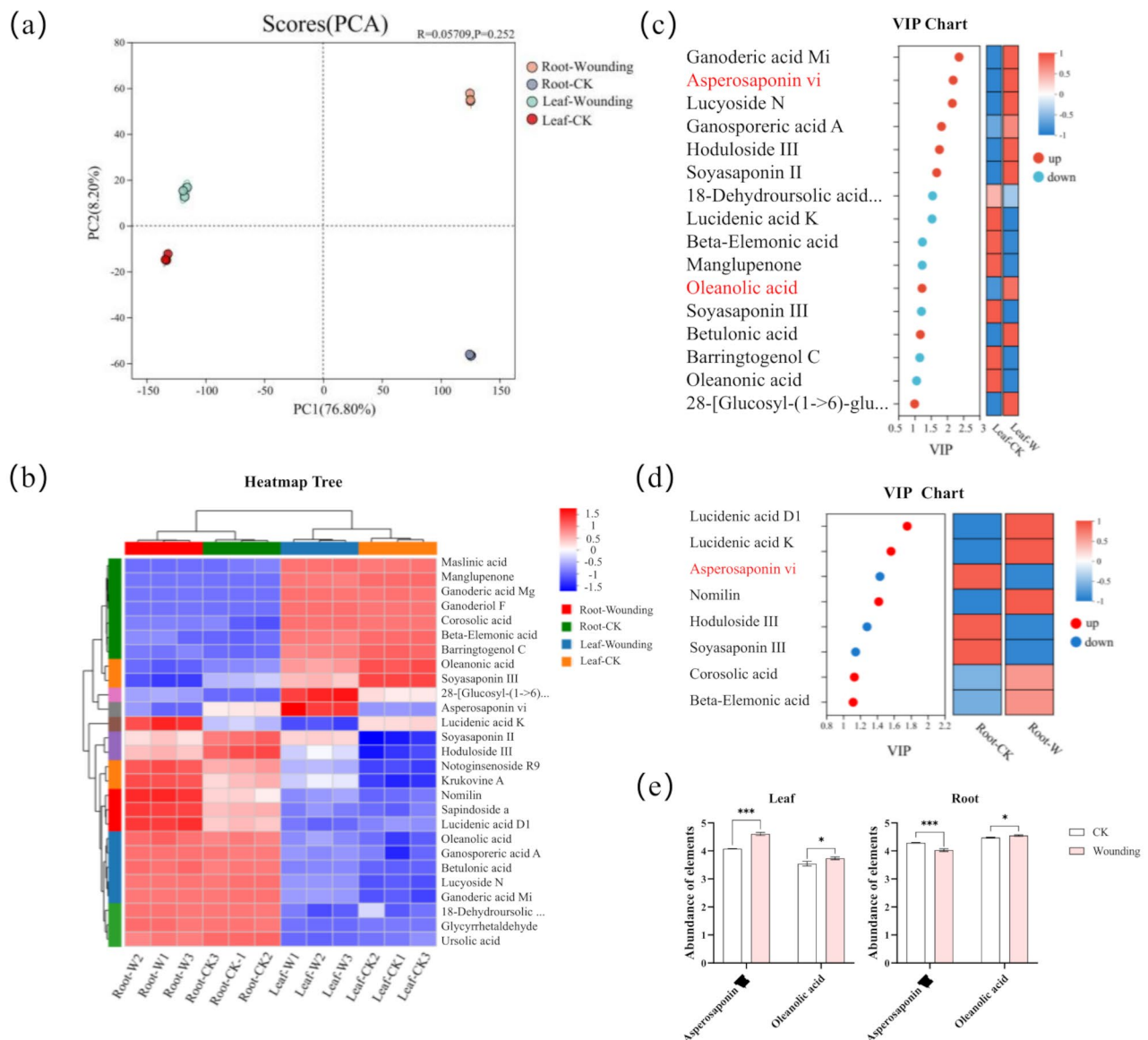


Fig. 4 Metabolite analysis of *D. asper* before and after wounding. **(a)** PCA plot. **(b)** Cluster heatmap. The heat map represents metabolites whose abundance is up-regulated, and blue represents metabolites whose abundance is down-regulated. **(c)** VIP plot of metabolites in leaves. The heat map represents metabolites whose abundance is up-regulated, and blue represents metabolites whose abundance is down-regulated. The red letters are triterpenoids. **(d)** VIP plot of metabolites in roots. The heat map represents metabolites whose abundance is up-regulated, and blue represents metabolites whose abundance is down-regulated. The red letters are triterpenoids. **(e)** Content of asperosaponin VI and oleanolic acid. Data represent the values of the mean \pm SE (standard error) of three replicates. Note Different lowercase letters indicate significant differences between treatments under the same indicator ($p < 0.05$)

control group (Fig. 4c, e). This suggests that asperosaponin VI may play a crucial role in *D. asper*'s resistance to mechanical damage. After leaf mechanical injury, the content of asperosaponin VI in the roots of *D. asper* significantly decreased, while *Oleanolic acid* content notably accumulated (Fig. 4d, e), suggesting that asperosaponin VI may be transferred from the roots to the leaves to help resist mechanical damage. These results indicate that mechanical injury can promote the accumulation of the stress-resistant component asperosaponin VI in *D. asper*.

Wounding increases the expression of *DaERF9* and genes involved in Asperosaponin VI synthesis

The results above indicate that *D. asper* resists external stress by increasing the accumulation of asperosaponin VI. qRT-PCR analysis of gene expression showed that the expression of the *DaERF9* gene was significantly upregulated after wounding, with the highest relative expression observed at 12 h post-injury, followed by 6 h post-injury. The expression of *DaERF9* exhibited an initial increase followed by a decrease over time (Fig. 5a). Meanwhile,

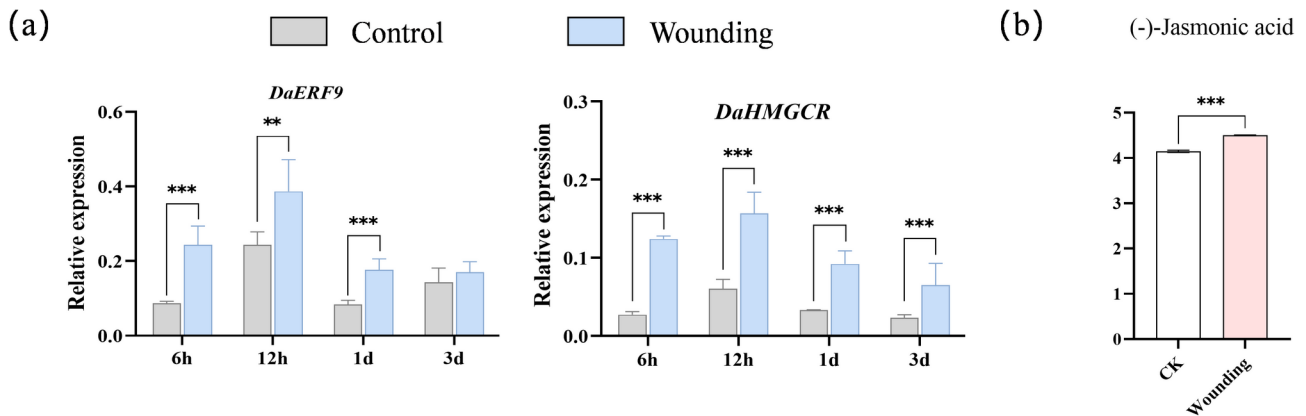


Fig. 5 Gene expression and JA content under wounding. **(a)** The gene express. **(b)** The JA content. Data represent the values of the mean \pm SE (standard error) of three replicates. Note Different lowercase letters indicate significant differences between treatments under the same indicator ($p < 0.05$)

compared to the control group, the expression of genes involved in the asperosaponin VI biosynthesis pathway, *DaHMGCR*, was significantly increased after injury. The expression trends of these genes also followed the pattern of an initial increase followed by a decrease (Fig. 5b). At the same time, the content of JA in *D. asper* after mechanical injury was significantly higher than in the control group (Fig. 5c). Based on these findings, it is speculated that *DaERF9* may regulate the expression of genes in the asperosaponin VI biosynthesis pathway by JA pathway, thereby promoting the synthesis of asperosaponin VI to respond to external stress.

DaERF9 binds to and activates the expression of *DaHMGCR*

Correlation analysis between the asperosaponin VI biosynthesis pathway genes and the *DaERF9* gene was conducted before and after mechanical injury. Before wounding, the expression of *DaERF9* demonstrated a significant positive correlation with key genes involved in asperosaponin VI biosynthesis, such as *DaAACT*, *DaHMGCR*, *DaHMGS*, *DaSS*, and *DaSE*. This indicates a potential regulatory relationship between *DaERF9* and the biosynthesis pathway under normal conditions. The correlation between *DaERF9* and *DaHMGCR* was the strongest, reaching 0.91. After wounding, *DaERF9* showed positive correlations with *DaHMGCR*, *DaHMGS*, and *DaSS*, with the strongest correlation with *DaHMGCR* at 0.73 (Fig. 6a). Based on these results, it is hypothesized that *DaHMGCR* is a downstream target gene of *DaERF9* in regulating the synthesis of asperosaponin VI. To verify this hypothesis, the full-length *DaHMGCR* gene (5883 bp) was obtained through chromosome walking, which contains five intronic regions, with the longest intron spanning 1638 base pairs (Supplemental Fig. 5a). Additionally, the full-length 1420 bp *DaHMGCR* gene promoter was cloned, and cis-acting element analysis revealed that this region contains three G-box binding motifs (Supplemental Fig. 5b). The LUC

results showed that the *Pro-DaHMGCR* and *DaERF9* combination injected into tobacco leaves emitted fluorescence, whereas the control group showed no fluorescence (Fig. 6b), indicating an interaction between *DaERF9* and *Pro-DaHMGCR*. Further verification through yeast one-hybrid assays showed that both the positive control group and the *DaERF9* plus *Pro-DaHMGCR* group exhibited blue coloration on yeast selective media (Fig. 6c), confirming the interaction between *DaERF9* and *Pro-DaHMGCR*. Based on these results, it can be concluded that *DaERF9* binds to the G-box in *Pro-DaHMGCR* to regulate the expression of the *DaHMGCR* gene.

Discussion and conclusion

Wounding-induced Asperosaponin VI biosynthesis and its association with the JA signaling

In previous studies conducted by our research group, it was demonstrated that MeJA treatment can promote the synthesis of asperosaponin VI. To investigate the regulatory mechanisms underlying asperosaponin VI biosynthesis, we screened the transcriptome of *D. asper* and identified the AP2/ERF family as closely associated with both JA signaling and asperosaponin VI synthesis [15]. Through phylogenetic tree and gene expression analysis, we identified that the *DaERF9* gene exhibits high homology with stress-responsive genes. Additionally, the expression level of *DaERF9* significantly increased under MeJA induction [22]. We hypothesize that *DaERF9* is a key regulatory gene involved in the biosynthesis of asperosaponin VI. Therefore, this study focuses on the cloning and functional verification of this gene, providing a foundational basis for elucidating the regulatory mechanisms and biosynthetic pathways of asperosaponin VI.

MeJA is a plant hormone that is widely involved in the regulation of plant secondary metabolites, particularly in the synthesis of triterpenoid saponins. MeJA promotes the synthesis of glycyrrhizin by inducing the expression of genes such as β -amyrin synthase (β -AS) and UGT

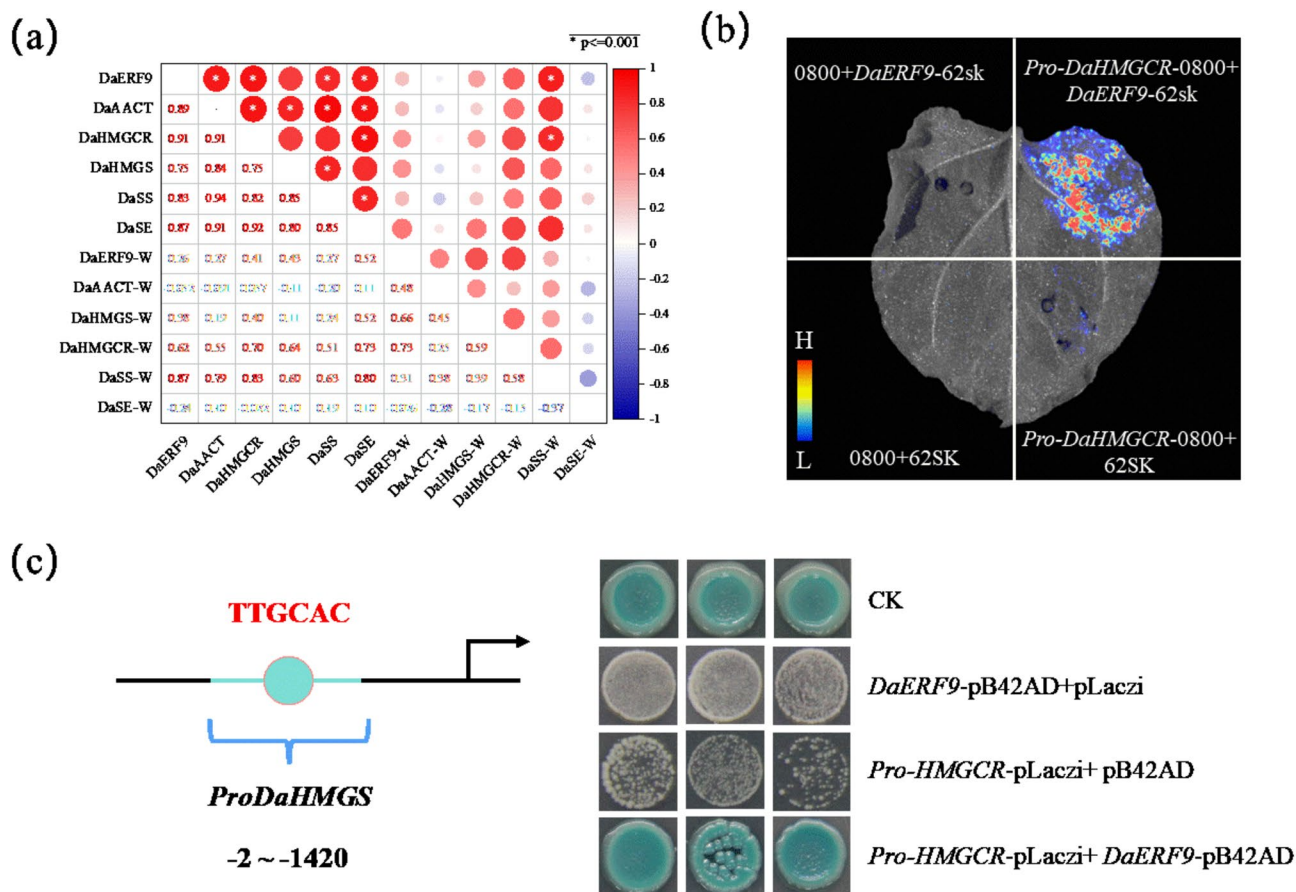


Fig. 6 Interaction analysis between *DaERF9* and *Pro-DaHMGR*. **(a)** Correlation analysis. The heat map represents metabolites whose abundance is up-regulated, and blue represents metabolites whose abundance is down-regulated. Where W represents the intermittent sample for mechanical damage treatment. **(b)** Dual-luciferase reporter assay. Red represents high fluorescence intensity, blue represents low fluorescence intensity. **(c)** Yeast one-hybrid assay. Data represent the values of the mean \pm SE (standard error) of three replicates. Note Different lowercase letters indicate significant differences between treatments under the same indicator ($p < 0.05$)

(uridine diphosphate glycosyltransferase) [23]. After MeJA treatment, the saponin content in jujube significantly increased, and the genes of several key enzymes in its biosynthesis pathway, such as HMGS, HMGR, and SE, were significantly activated [24]. MeJA can significantly upregulate the expression of several key enzyme genes, such as HMGR, SS, and UGT, thereby promoting the synthesis of triterpenoid compounds in *Polygonum cuspidatum* [25]. In *D. asper*, MeJA treatment significantly increases the expression of genes involved in the biosynthesis pathway of asperosaponin VI, such as AACT, HMGR, and HMGS, thereby promoting the accumulation of asperosaponin VI content [15]. By studying the mechanism of MeJA's effect on triterpenoid saponin synthesis, it can provide theoretical support for the accumulation of secondary metabolites in medicinal plants and offer important technical approaches for the industrial production of triterpenoid saponins.

The role of MeJA in plant mechanical injury, especially in the aspect of secondary metabolite production for

stress resistance, is of significant importance. MeJA can significantly promote the synthesis of various secondary metabolites, such as terpenoids, flavonoids, phenolic compounds, and volatile organic compounds. The terpenoids and alkaloids synthesized by plants in response to MeJA have natural antimicrobial and antiviral properties, which effectively defend against pathogen infection at the wound site [26]. At the same time, MeJA can also activate the plant's antioxidant enzyme system, reducing oxidative damage caused by mechanical injury [27]. MeJA enhances the plant's resistance to pests and diseases during mechanical injury by promoting the synthesis of secondary metabolites. For example, MeJA can induce the production of volatile organic compounds (VOCs) in plants. These compounds not only attract predatory natural enemies through their aroma to control pests but also inhibit the growth and spread of certain pathogenic microorganisms [28]. MeJA promotes the accumulation of secondary metabolites by activating the expression of plant defense-related genes. These

genes include those involved in antioxidant responses, cell wall reinforcement, and the synthesis of defense proteins [29]. In our results, mechanical injury promoted the content of jasmonic acid and asperosaponin VI in *D. asper*. It is speculated that the JA signaling pathway plays an important role in the synthesis of asperosaponin VI. In this way, MeJA enhances the overall stress resistance of plants, particularly by accumulating secondary metabolites to cope with the various stresses induced by mechanical injury. In summary, MeJA plays a crucial role in plant mechanical injury by regulating the synthesis and accumulation of secondary metabolites. This process enhances plant resistance, protects against pathogen invasion, reduces oxidative damage, and improves the plant's ability to adapt to external stresses by strengthening its natural defense system.

Wounding is a common form of abiotic stress in plants, and it can induce the synthesis of secondary metabolites, including triterpenoid saponins, by activating signaling pathways. Mechanical damage rapidly activates the JA signaling pathway, inducing the expression of genes related to the synthesis of triterpenoid saponins, such as HMGR and SS, thereby promoting the synthesis of saponins in *Elaeocarpus sylvestris* and *Illicium henryi* [30]. Mechanical injury induces the release of endogenous MeJA in plants, thereby activating the expression of a series of defense-related genes, including those associated with the synthesis of triterpenoid saponins. Exogenous MeJA, on the other hand, enhances the plant's response to mechanical injury through long-distance signaling, increasing the synthesis of secondary metabolites. This synergistic effect not only strengthens the plant's stress resistance but also significantly improves the yield of secondary metabolites such as triterpenoid saponins [31, 32]. In *D. asper*, exogenous MeJA treatment promotes the accumulation of asperosaponin VI content and significantly increases the expression of genes involved in the synthesis pathway of asperosaponin VI. At the same time, after mechanical injury, the content of asperosaponin VI and its precursor, oleanolic acid, significantly increases, activating the synthesis pathway of asperosaponin VI. This indicates that mechanical injury can promote the synthesis of asperosaponin VI in *D. asper*, suggesting that asperosaponin VI may be a key resistance component in the plant's response to mechanical damage.

***D. asper* resists mechanical damage by eliminating ROS**

Mechanical injury triggers the production of reactive oxygen species (ROS), creating an oxidative stress within the plant, which, to some extent, helps activate defense mechanisms. However, excessive accumulation of ROS can lead to cellular damage, prompting plants to rely on their antioxidant systems to regulate ROS levels and prevent excessive oxidation from harming the cells.

Mechanical injury results in the overproduction of ROS, thereby inducing oxidative stress. For example, in sunflower seedlings, mechanical injury significantly increases ROS production, leading to higher levels of lipid peroxidation products like MDA, which is a typical marker of oxidative stress [33]. Enzymatic antioxidants such as SOD and POD effectively scavenge ROS, thereby preventing oxidative damage to cells. These enzymes play a crucial role in maintaining cellular homeostasis by detoxifying reactive oxygen species and protecting the plant from oxidative stress-induced damage [34, 35]. Our results indicate that after mechanical injury to *D. asper* leaves, the MDA content in the leaves significantly increased, suggesting that the plant experienced stress and oxidative stress. Meanwhile, the enzymatic antioxidant activities of SOD and POD were significantly elevated, confirming that *D. asper* mounts a resistance response to mechanical injury. Additionally, the ROS accumulation triggered by mechanical injury may promote the synthesis of plant secondary metabolites, such as terpenes and other antioxidant compounds. These secondary metabolites can enhance the plant's ability to adapt to external stresses. In *Catharanthus roseus*, mechanical injury also leads to increased ROS content, which helps reduce oxidative damage by boosting the synthesis of secondary metabolites [36]. In *Daucus carota* (carrot), the significant accumulation of secondary metabolites can reduce the damage caused by ROS to cells and mitigate external stress. These secondary metabolites act as protective compounds, enhancing the plant's ability to resist oxidative damage and improve its overall stress tolerance [37]. In this study, mechanical injury significantly increased the expression of genes involved in the synthesis pathway of asperosaponin VI and the accumulation of asperosaponin VI content. It is speculated that asperosaponin VI serves as a hallmark component for *D. asper* in resisting damage, mitigating the harm caused by mechanical injury by eliminating oxidative damage.

***DaERF9* enhances the biosynthesis of Asperosaponin VI through the regulation of *DaHMGR* expression**

The ERF transcription factor, a member of the AP2/ERF superfamily, is closely related to the regulation of plant secondary metabolism, particularly playing an important role in promoting triterpenoid saponin synthesis. ERF transcription factors activate the transcription of key genes involved in the triterpenoid saponin biosynthesis pathway, such as HMGR, FPS, SS, and UGT genes, by directly binding to the promoters of these genes, thereby enhancing the synthesis of triterpenoid saponins [38]. The precursor of glycyrrhizin saponins, β -amyrin, is synthesized through a series of enzymatic reactions, including enzymes such as *CYP88D6*, *CYP72A15*, and *CYP93E6*. Additionally, the gene expression regulation

in the biosynthesis pathway of glycyrrhizin saponins involves various transcription factors, such as MYB, FKR, bHLH, and ERF [39]. In *Panax ginseng*, studies have shown that *PgERF120* significantly enhances the accumulation of ginsenosides by binding to the promoters of key enzymes in triterpenoid saponin synthesis, such as HMGR and SQS [40]. Similar to our results, the content of the precursor oleanolic acid for the synthesis of asperosaponin VI significantly accumulated in transgenic *Arabidopsis* with *DaERF9*. At the same time, the key enzyme genes involved in the synthesis of asperosaponin VI were significantly upregulated, confirming that *DaERF9* regulates the synthesis of asperosaponin VI. After MeJA treatment, only the *DaHMGR* gene in transgenic *DaERF9* showed a significant upregulation, suggesting that *DaHMGR* is a downstream target gene regulated by *DaERF9*. Using gene scaling after mechanical injury for correlation analysis, the most significantly correlated gene with *DaERF9* was identified as *DaHMGR*. This confirms that *DaHMGR* is a downstream target gene regulated by *DaERF9*.

ERF transcription factors regulate the synthesis of secondary metabolites by binding to the G-box in target genes. In *Litsea cubeba*, *LcERF19* binds to the GCC box element in the promoter of *LcTPS42*, promoting its activity. This activation enhances the biosynthesis of citronellal and nerolidol by upregulating the expression of *LcTPS42* [41]. In the JA signaling pathway, ERF transcription factors such as *ERF109* can bind to the G-box sequence in the promoters of JA-responsive genes, thereby regulating the expression of these genes. This, in turn, affects the synthesis of plant secondary metabolites like anthocyanins [42]. In *Catharanthus roseus*, ERF transcription factors bind to the G-box in the promoters of key genes, thereby regulating the biosynthesis of vincristine [43]. In this study, the *DaHMGR* promoter was obtained through chromosome walking, and a cis-element analysis revealed the presence of multiple G-box binding elements. The interaction between *DaERF9* and the *DaHMGR* promoter was validated using LUC and Y1H assays. Thus, it was concluded that *DaERF9* promotes the biosynthesis of asperosaponin VI by binding to the G-box elements in the *DaHMGR* promoter.

Based on the above, *DaERF9* regulates the key enzyme genes involved in the synthesis of asperosaponin VI by responding to JA, significantly upregulating them under mechanical injury. Furthermore, *DaERF9* can bind to the G-box in the *DaHMGR* promoter, regulating the synthesis of asperosaponin VI under mechanical injury, thereby helping *D. asper* resist stress.

Abbreviations

AACT	Acetyl-CoA acetyltransferase
HMGS	3-Hydroxy-3-methylglutaryl-CoA synthase
HMGR	Hydroxy-3-methylglutaryl-CoA reductase

JA	Jasmonic acid
MDA	Malondialdehyde
MeJA	Methyl jasmonate
POD	Peroxidase
ROS	Reactive oxygen species
SE	Squalene epoxidase
SOD	Superoxide dismutase
SS	Squalene synthase

Supplementary Information

The online version contains supplementary material available at <https://doi.org/10.1186/s12870-025-06576-w>.

Supplementary Material 1

Acknowledgements

We are grateful for the founding support provided.

Author contributions

Huanhuan Yang: Responsible for the conception and design of the research, leading the data analysis and interpretation, and writing the initial draft of the manuscript. Jiao Xu: Responsible for obtaining experimental data and experimental design, participating in data analysis, and making significant contributions to the revision of the manuscript. Chunyun Xu: Participated in obtaining and analyzing experimental data, assisting in verifying and interpreting research results. Guang Zhou: Responsible for data analysis in the research, participating in data processing and interpretation. Tao Zhou*: Responsible for the overall design and guidance of the research, participating in data interpretation and manuscript revision, and serving as the corresponding author to communicate with the journal. Chenghong Xiao*: Responsible for the conception and design of the research, participating in data analysis and interpretation, guiding the writing and revision of the manuscript, and serving as the corresponding author to communicate with the journal. All authors have approved the final version of the manuscript and are accountable for their individual contributions, ensuring the accuracy and integrity of the research. The corresponding authors (denoted by *) are responsible for communicating with the journal's editorial office regarding peer review and publication matters.

Funding

This work was supported by the National Key R&D Program of China (2023YFC3503803) and National Natural Science Foundation of China (82160725).

Data availability

Data is provided within the manuscript or supplementary information files.

Declarations

Ethics approval and consent to participate

The wild seed collection and the trial conducted in this study were in no violation of any legislation, including the IUCN Policy Statement on Research Involving Species at Risk of Extinction and the Convention on the Trade in Endangered Species of Wild Fauna and Flora. The wild seeds of the two ecotypes were identified by Prof. Xiao-Chenghong, the collection was permitted by the local government of the aforementioned sites.

Consent for publication

Not applicable.

Competing interests

The authors declare no competing interests.

Received: 5 February 2025 / Accepted: 17 April 2025

Published online: 09 May 2025

References

- Wei F, Ruan B, Dong J, Yang B, Zhang G, Kelvin YW, Wang H, Cao W, Wang Y. Asperosaponin VI Inhibition of DNMT alleviates GPX4 suppression-mediated osteoblast ferroptosis and diabetic osteoporosis. *J ADV RES* 2024. 11:036.
- Mo Y, Yang Y, Zeng J, Ma W, Guan Y, Guo J, Wu X, Liu D, Feng L, Jia X, et al. Enhancing the biopharmacological characteristics of Asperosaponin VI: unveiling dynamic Self-Assembly phase transitions in the Gastrointestinal environment. *Int J Nanomed*. 2023;18:7335–58.
- Huang J, Liang X, Zhao M, Zhang Y, Chen Z. Metabolomics and network Pharmacology reveal the mechanism of antithrombotic effect of Asperosaponin VI. *BIOMED PHARMACOTHER*. 2024;173:116355.
- Skala E, Szopa A. Dipsacus and Scabiosa Species-The source of specialized metabolites with high biological relevance: A review. *Molecules* 2023;(28):3754.
- Ni Q, Chen Z, Zheng Q, Xie D, Li JJ, Cheng S, Ma X. Epithelial V-like antigen 1 promotes hepatocellular carcinoma growth and metastasis via the ERBB-P13K-AKT pathway. *CANCER SCI*. 2020;111(5):1500–13.
- Luo JF, Yu Y, Liu JX. Mechanism of Asperosaponin VI related to EGFR/MMP9/AKT/P13K pathway in treatment of rheumatoid arthritis. *CHIN J INTEGR MED* 2025;31(2):131–141.
- Gastaldo C, Lipko A, Motsch E, Adam P, Schaeffer P, Rohmer M. Biosynthesis of isoprene units in *Euphorbia lathyris* laticifers vs. Other tissues: MVA and MEP pathways, compartmentation and putative endophytic Fungi contribution. *Molecules*. 2019;24(23):4322.
- Li C, Zha W, Li W, Wang J, You A. Advances in the biosynthesis of terpenoids and their ecological functions in plant resistance. *INT J MOL SCI* 2023, 24(14):11561.
- Liu X, Xu Y, Di J, Liu A, Jiang J. The triterpenoid saponin content difference is associated with the two type oxidosqualene cyclase gene copy numbers of *Pulsatilla chinensis* and *Pulsatilla Cernua*. *FRONT PLANT SCI*. 2023;14:1144738.
- Yu J, Yu Z, Wang Y, Bao J, Zhu K, Yuan T, Zhang H. Triterpenoids and triterpenoid saponins from *Dipsacus Asper* and their cytotoxic and antibacterial activities. *Phytochemistry*. 2019;162:241–9.
- Tao Y, Chen L, Yan J. Traditional uses, processing methods, phytochemistry, Pharmacology and quality control of *Dipsacus Asper* wall. *Ex C.B. Clarke: A review. J ETHNOPHARMACOL*. 2020;258:112912.
- Deng B, Huang Z, Ge F, Liu D, Lu R, Chen C. An AP2/ERF family transcription factor PnERF1 Raised the biosynthesis of saponins in *Panax Notoginseng*. *J PLANT GROWTH REGUL*. 2017;36(3):691–701.
- Huang X, Zhang W, Liao Y, Ye J, Xu F. Contemporary Understanding of transcription factor regulation of terpenoid biosynthesis in plants. *Planta*. 2023;259(1):2.
- Li Y, Lin Y, Jia B, Chen G, Shi H, Xu R, Li X, Tang J, Tang Q, Zhang G, et al. Transcriptome analysis reveals molecular mechanisms underlying Methyl Jasmonate-mediated biosynthesis of Protopanaxadiol-type saponins in *Panax Notoginseng* leaves. *J PLANT BIOL*. 2022;65(1):29–41.
- Xu J, Hu Z, He H, Ou X, Yang Y, Xiao C, Yang C, Li L, Jiang W, Zhou T. Transcriptome analysis reveals that jasmonic acid biosynthesis and signaling is associated with the biosynthesis of Asperosaponin VI in *Dipsacus Asperoides*. *FRONT PLANT SCI*. 2022;13:1022075.
- Chen X, Hudson GA, Mineo C, Amer B, Baidoo E, Crowe SA, Liu Y, Keasling JD, Scheller HV. Deciphering triterpenoid saponin biosynthesis by leveraging transcriptome response to Methyl jasmonate elicitation in *Saponaria vaccaria*. *NAT COMMUN*. 2023;14(1):7101.
- Kim Y, Kim YB, Kim JK, Kim S, Park SU. Molecular cloning and characterization of mevalonic acid (MVA) pathway genes and triterpene accumulation in *Panax ginseng*. *J KOREAN SOC APPL BI*. 2014;57(3):289–95.
- Mertens J, Pollier J, Vanden Bossche R, Lopez-Vidriero I, Franco-Zorrilla JM, Goossens A. The bHLH transcription factors TSAR1 and TSAR2 regulate triterpene saponin biosynthesis in *Medicago truncatula*. *Plant Physiology/Plant Physiol*. 2015;170(1):194–210.
- Zhang X, Ge F, Deng B, Shah T, Huang Z, Liu D, Chen C. Molecular Cloning and Characterization of PnbHLH1 Transcription Factor in *Panax notoginseng*. *MOLECULES* 2017, 22(8).
- Yuanyuan Z, Xiaojing D, Ya L, Huaijun T, Bing D, Wenjin S. Research Progress of Molecular Biology of *Arabidopsis thaliana*. 2018;34 (30):56–62.
- Zhang X, Henriques R, Lin S, Niu Q, Chua N. Agrobacterium-mediated transformation of *Arabidopsis thaliana* using the floral dip method. *NAT PROTOC*. 2006;1(2):641–6.
- Yang H, Xu J, Xu C, Zhou G, Zhou T, Xiao C. Molecular insights into DaERF108-mediated regulation on Asperosaponin VI biosynthesis under cold tolerance in *Dipsacus Asper*. *Plant Physiol Biochem*. 2025;221:109632.
- Akhatou I, González-Domínguez R, Fernández-Recamales Á. Investigation of the effect of genotype and agronomic conditions on metabolomic profiles of selected strawberry cultivars with different sensitivity to environmental stress. *PLANT PHYSIOL BIOCH*. 2016;101:14–22.
- Wen C, Zhang Z, Shi Q, Duan X, Du J, Wu C, Li X. Methyl Jasmonate- and Salicylic Acid-Induced transcription factor ZJWRKY18 regulates triterpenoid accumulation and salt stress tolerance in jujube. *INT J MOL SCI* 2023, 24(4).
- Tian R, Gu W, Gu Y, Geng C, Xu F, Wu Q, Chao J, Xue W, Zhou C, Wang F. Methyl jasmonate promote protostane triterpenes accumulation by up-regulating the expression of squalene epoxidases in *Alisma orientale*. *Sci Rep*. 2019;9(1):18139.
- Li S, Zhang P, Zhang M, Fu C, Zhao C, Dong Y, Guo A, Yu L. Transcriptional profile of *Taxus chinensis* cells in response to Methyl jasmonate. *BMC Genomics*. 2012;13(1):295.
- Shi R, Yu J, Chang X, Qiao L, Liu X, Lu L. Recent advances in research into jasmonate biosynthesis and signaling pathways in agricultural crops and products. *Processes*. 2023;11(3):736.
- Sobhy SE, Al-Huqail AA, Khan F, Abd-Allah RG, El-Sheikh MA, Ahmed AR, Saleh AA, Hafez EE. Elicitation of Salicylic acid and Methyl jasmonate provides molecular and physiological evidence for potato susceptibility to infection by *Erwinia carotovora* subsp. *carotovora*. *Heliyon*. 2024;10(10):30929.
- Xia C, Xue W, Li Z, Shi J, Yu G, Zhang Y. Presenting the secrets: exploring endogenous defense mechanisms in chrysanthemums against aphids. *Horticulturae*. 2023;9(8):937.
- Xie H, Yu M, Cheng X. Leaf non-structural carbohydrate allocation and C:N:P stoichiometry in response to light acclimation in seedlings of two subtropical shade-tolerant tree species. *PLANT PHYSIOL BIOCH*. 2018;124:146–54.
- Balusamy D, Rahimi S, Sukweenadhi J, Kim Y, Yang D. Exogenous Methyl jasmonate prevents necrosis caused by mechanical wounding and increases terpenoid biosynthesis in *Panax ginseng*. *Plant Cell Tissue Organ Cult (PCTOC)*. 2015;123(2):341–8.
- James T, Tugizimana F, Steenkamp A, Dubery IA. Metabolomic analysis of Methyl Jasmonate-Induced triterpenoid production in the medicinal herb *Centella asiatica* (L.) urban. *Molecules*. 2013;18(4):4267–81.
- Chaki M, Valderrama R, Fernández-Ocaña M, Carreras A, Gómez-Rodríguez V, Pedrajas R, Begara-Morales C, Sánchez-Calvo B, Luque F, Leterrier M, et al. Mechanical wounding induces a nitrosative stress by down-regulation of GSNO reductase and an increase in S-nitrosothiols in sunflower (*Helianthus annuus*) seedlings. *J EXP BOT*. 2011;62(6):1803–13.
- Hasanuzzaman M, Bhuyan MHMB, Zulfiqar F, Raza A, Mohsin SM, Mahmud JA, Fujita M, Fotopoulos V. Reactive oxygen species and antioxidant defense in plants under abiotic stress: revisiting the crucial role of a universal defense regulator. *Antioxidants*. 2020;9(8):681.
- Abdulfatah HF. Non-Enzymatic antioxidants in stressed plants: A review. *J Univ Anbar Pure Sci* 2022,(16),(2):25–37.
- Chen Q, Jin Y, Guo X, Xu M, Wei G, Lu X, Tang Z. Metabolomic responses to the mechanical wounding of *Catharanthus roseus* 'upper leaves'. *PEERJ* 2023, 11:14539.
- Jacobo-Velázquez DA, González-Agüero M, Cisneros-Zevallos L. Cross-talk between signaling pathways: the link between plant secondary metabolite production and wounding stress response. *SCI REP-UK*. 2015;5(1):8608.
- Zheng H, Fu X, Shao J, Tang Y, Yu M, Li L, Huang L, Tang K. Transcriptional regulatory network of high-value active ingredients in medicinal plants. *TRENDS PLANT SCI*. 2023;28(4):429–46.
- Yang J, Yan H, Liu Y, Da L, Xiao Q, Xu W, Su Z. GURFAP: A platform for gene function analysis in *Glycyrrhiza uralensis*. *FRONT GENET* 2022, 13.
- Jiang Y, Zhang Q, Zeng Z, Wang Y, Zhao M, Wang K, Zhang M. The AP2/ERF transcription factor PgERF120 regulates ginsenoside biosynthesis in ginseng. *Biomolecules*. 2024;14(3):345.
- Wang M, Gao M, Zhao Y, Chen Y, Wu L, Yin H, Xiong S, Wang S, Wang J, Yang Y, et al. LcERF19, an AP2/ERF transcription factor from *Litsea Cubeba*, positively regulates geraniol and Neral biosynthesis. *Hortic Res*. 2022;9:c93.
- Li J, Yu G, Wang X, Guo C, Wang Y, Wang X. Jasmonic acid plays an important role in mediating retrograde signaling under mitochondrial translational stress to balance plant growth and defense. *Plant Communications*. 2025;6(1):101133.

43. Paul P, Singh SK, Patra B, Liu X, Pattanaik S, Yuan L. Mutually regulated AP2/ERF gene clusters modulate biosynthesis of specialized metabolites in Plants1[OPEN]. *Plant PhysiologyPlant Physiol.* 2019;182(2):840–56.

Publisher's note

Springer Nature remains neutral with regard to jurisdictional claims in published maps and institutional affiliations.